

RESEARCH ARTICLE

# Expression of Phosphoinositide-Specific Phospholipase C Isoforms in Native Endothelial Cells

Delphine M. Béziau<sup>1,2</sup>, Fanny Toussaint<sup>1,2</sup>, Alexandre Blanchette<sup>1</sup>, Nour R. Dayeh<sup>1,4</sup>, Chimène Charbel<sup>1,3</sup>, Jean-Claude Tardif<sup>1,4</sup>, Jocelyn Dupuis<sup>1,4</sup>, Jonathan Ledoux<sup>1,2,3,4\*</sup>

**1** Research Center, Montreal Heart Institute, Montreal, Qc, Canada, **2** Department of Molecular and Integrative Physiology, Université de Montréal, Montreal, Qc, Canada, **3** Department of Pharmacology, Université de Montréal, Montreal, Qc, Canada, **4** Department of Medicine, Université de Montréal, Montreal, Qc, Canada

\* [jonathan.ledoux@umontreal.ca](mailto:jonathan.ledoux@umontreal.ca)



**OPEN ACCESS**

**Citation:** Béziau DM, Toussaint F, Blanchette A, Dayeh NR, Charbel C, Tardif J-C, et al. (2015) Expression of Phosphoinositide-Specific Phospholipase C Isoforms in Native Endothelial Cells. PLoS ONE 10(4): e0123769. doi:10.1371/journal.pone.0123769

**Academic Editor:** Mohamed Trebak, Penn State Hershey College of Medicine, UNITED STATES

**Received:** December 4, 2014

**Accepted:** February 25, 2015

**Published:** April 13, 2015

**Copyright:** © 2015 Béziau et al. This is an open access article distributed under the terms of the [Creative Commons Attribution License](https://creativecommons.org/licenses/by/4.0/), which permits unrestricted use, distribution, and reproduction in any medium, provided the original author and source are credited.

**Data Availability Statement:** All relevant data are within the paper.

**Funding:** This study was support through studentship and salary grants: Université de Montréal - Fanny Toussaint, Nour R. Dayeh; Société Québécois d'Hypertension Artérielle (SQHA) - Delphine M. Béziau and Fanny Toussaint; Fonds de Recherche du Québec - Santé (FRQS) - Jonathan Ledoux; Canadian Institutes of Health Research (CIHR) - Jonathan Ledoux; The Canada Foundation for Innovation (CFI) - Jonathan Ledoux; Heart and Stroke Foundation of Canada (HSFC) - Jonathan

## Abstract

Phospholipase C (PLC) comprises a superfamily of enzymes that play a key role in a wide array of intracellular signalling pathways, including protein kinase C and intracellular calcium. Thirteen different mammalian PLC isoforms have been identified and classified into 6 families (PLC- $\beta$ ,  $\gamma$ ,  $\delta$ ,  $\epsilon$ ,  $\zeta$  and  $\eta$ ) based on their biochemical properties. Although the expression of PLC isoforms is tissue-specific, concomitant expression of different PLC has been reported, suggesting that PLC family is involved in multiple cellular functions. Despite their critical role, the PLC isoforms expressed in native endothelial cells (ECs) remains undetermined. A conventional PCR approach was initially used to elucidate the mRNA expression pattern of PLC isoforms in 3 distinct murine vascular beds: mesenteric (MA), pulmonary (PA) and middle cerebral arteries (MCA). mRNA encoding for most PLC isoforms was detected in MA, MCA and PA with the exception of  $\eta$ 2 and  $\beta$ 2 (only expressed in PA),  $\delta$ 4 (only expressed in MCA),  $\eta$ 1 (expressed in all but MA) and  $\zeta$  (not detected in any vascular beds tested). The endothelial-specific PLC expression was then sought in freshly isolated ECs. Interestingly, the PLC expression profile appears to differ across the investigated arterial beds. While mRNA for 8 of the 13 PLC isoforms was detected in ECs from MA, two additional PLC isoforms were detected in ECs from PA and MCA. Co-expression of multiple PLC isoforms in ECs suggests an elaborate network of signalling pathways: PLC isoforms may contribute to the complexity or diversity of signalling by their selective localization in cellular microdomains. However in situ immunofluorescence revealed a homogeneous distribution for all PLC isoforms probed ( $\beta$ 3,  $\gamma$ 2 and  $\delta$ 1) in intact endothelium. Although PLC isoforms play a crucial role in endothelial signal transduction, subcellular localization alone does not appear to be sufficient to determine the role of PLC in the signalling microdomains found in the native endothelium.

Ledoux. The funders had no role in study design, data collection and analysis, decision to publish, or preparation of the manuscript.

**Competing Interests:** The authors declare that no competing interests exist.

## Introduction

Vascular endothelium, a thin-cell monolayer lining blood vessels walls, is ideally positioned to detect and transduce biochemical and physical information. Endothelial cells (ECs) are essential regulators of vascular tone, cellular adhesion and vascular smooth muscle cell (SMC) proliferation. The wide variety of stimuli sensed by ECs necessitates an intricate web of intracellular signalling components, including phosphoinositide-signalling involving phospholipases C (PLC) as main players.

PLC are calcium ( $\text{Ca}^{2+}$ )-dependent phosphodiesterases that hydrolyze phosphatidyl-inositol biphosphate ( $\text{PIP}_2$ ) into 1,2-diacylglycerol (DAG) plus inositol trisphosphate ( $\text{IP}_3$ ) [1,2]. Once generated,  $\text{IP}_3$  quickly diffuses in the cytoplasm and activates  $\text{IP}_3$  receptors ( $\text{IP}_3\text{R}$ ) located on the endoplasmic reticulum (ER) membrane, evoking a rapid release of  $\text{Ca}^{2+}$  into the cytoplasm. PLC can also regulate several cellular functions through DAG production, via activation of protein kinase C [3] and through modulation of  $\text{PIP}_2$  levels [4]. To date, a total of 13 mammalian PLC isoforms have been identified and classified into 6 families:  $\beta(1-4)$ ,  $\gamma(1-2)$ ,  $\delta(1,3,4)$ ,  $\epsilon$ ,  $\zeta$  and  $\eta(1-2)$  [5]. The PLC families possess distinct mechanisms of activation. For example,  $\text{PLC}\beta$  isoforms are activated by  $G\alpha$  and  $G\beta/\gamma$  subunits of heterotrimeric G proteins whereas  $\text{PLC}\gamma$  isoforms are activated by tyrosine kinase receptors and  $\text{PLC}\epsilon$  can be activated by both [5]. PLC isoforms can also be distinguished by their molecular weights,  $\text{Ca}^{2+}$ -sensitivity and subcellular localization: together, these suggest that each isoform might have a specific role in the modulation of physiological responses and this is further supported by several studies using knockout animal models [5–8]. For example,  $\text{PLC}\epsilon$ -null mice display abnormal development of the aortic and pulmonary valves [9]. The absence of  $\text{PLC}\beta 2$  expression leads to decreased intracellular calcium release and superoxide production in neutrophils [10]. These studies strengthened the notion that each PLC isoform has a specific and complementary role in physiology.

Downstream of PLC activation,  $\text{IP}_3\text{R}$ -dependent  $\text{Ca}^{2+}$  release is a key player in endothelial function. Indeed, these endothelial intracellular  $\text{Ca}^{2+}$  dynamics play a major role in the generation of vasoregulatory signals [11–14]. Although highly dynamic, endothelial  $\text{Ca}^{2+}$  is finely tuned, as expected for a process with a significant functional impact. An increasing body of evidence suggests that spatially restricted  $\text{Ca}^{2+}$  signals are essential regulators of endothelial function. Of the endothelial local  $\text{Ca}^{2+}$  signals characterized,  $\text{Ca}^{2+}$  pulsars are spontaneous  $\text{IP}_3\text{R}$ -dependent  $\text{Ca}^{2+}$  release events that occur within the myoendothelial projection (MEP) [11]. Although our current knowledge regarding the regulation of spatially-localized  $\text{Ca}^{2+}$  signalling in the endothelium is limited, the involvement of  $\text{IP}_3/\text{IP}_3\text{Rs}$  indicate a role for PLCs in the control of  $\text{Ca}^{2+}$  signals such as pulsars. A better understanding of the expression and subcellular localization of PLCs in native ECs is necessary.

Cell-specific expression of individual PLCs is believed to be involved in modulating particular functions. Roles for  $\text{PLC}\beta 3$  [15],  $\gamma 1$  [16] and  $\delta$  [17] have been reported in ECs and the expression of PLC isoforms was recently examined in human umbilical vein endothelial cells (HUVECs) [18]. However, placing ECs in culture results in phenotypic changes [19], including the loss of MEP and  $\text{Ca}^{2+}$  pulsars, suggesting that the regulatory pathways might be altered as well. Hence, the expression profile of PLCs and the associated signalling pathways may differ between HUVECs and native ECs. Endothelium is a specialized tissue whose functions vary depending on the vascular bed, suggesting that PLC expression might also vary from one vascular bed to the other [20–22]. Therefore, it is crucial to determine the expression and subcellular distribution of PLC isoforms in native ECs from different vascular beds. In this study, we determined the expression of PLC isoforms in murine ECs freshly isolated from mesenteric (MAECs), pulmonary (PAECs) and middle cerebral arteries (MCAECs).

## Materials and Methods

### Tissue preparation

All animal manipulations were performed in accordance with the Canadian Council on Animal Care guidelines. The Montreal Heart Institute Animal Research Ethics Committee approved all animal studies (Protocol number: 2011-33-01). Resistance arteries: (3<sup>rd</sup> or 4<sup>th</sup> order MA, PA and MCA) were isolated from 3–4 months old C57BL/6 mice. Prior to experimentation, arteries were carefully cleaned of adipose and connective tissue in cooled HEPES solution.

### Molecular biology

Total RNA from MA, PA and MCA was extracted using RNeasy Micro kits (Qiagen). As control, total RNA was isolated from brain and testis using RNeasy Lipid tissue Mini Kit (Qiagen) and from blood using QIAmp RNA blood Mini kit (Qiagen). The purity and concentration of RNA were assessed using a Nanodrop spectrophotometer. Next, reverse transcription was performed using iScript kits (Bio-Rad) according to manufacturer's instructions. Primers (Table 1) and 5 ng of cDNA were used for PCR amplification in a final volume of 25  $\mu$ l. Following denaturation at 94°C, 45 cycles of DNA amplification were performed using Taq DNA polymerase (Invitrogen) at 94°C for 45 sec, 55°C for 30 sec and 72°C for 90 sec. A final extension step was performed for 10 min at 72°C. Electrophoresis of amplicons on 3% ethidium bromide stained agarose gels was carried out. PCR product sizes were estimated using the Gene ruler low range DNA ladder (Thermoscientific) and compared to theoretical amplicon size ( $n \geq 3$ , Table 1).

For quantitative real-time PCR (qPCR), ECs were freshly isolated from MA, PA and MCA as previously described by Socha et al [23]. Cell dissociation was performed in a tube containing 137 mM NaCl, 5.6 mM KCl, 1 mM MgCl<sub>2</sub>, 10mM HEPES, 10 mM glucose, 2 mM CaCl<sub>2</sub>, 1.0 mg/ml DTT, 0.1% BSA and with enzymes 0.62mg/ml (MAECs) or 0.31mg/ml (PAECs and MCAECs) papain (Sigma, P4762), 1.5mg/ml (MAECs) or 0.75mg/ml (PAECs and MCAECs) collagenase (Sigma, C8051). Arterial segments were incubated in digestion solution for 25 min at 37°C followed by a triple wash in enzyme-free solution and then gently triturated. SMC-deprived EC tubes were visually identified with a Zeiss Axiovert A1 microscope and individually

**Table 1. List of primer couples for PLC isoforms.**

Gene	Forward (5' → 3')	Reverse (5' → 3')	Amplicon size
PLC $\beta$ 1	CTGAGCGGAGAAGAAAATGG	ACACAGCGACATCCAGACAG	185
PLC $\beta$ 2	TCAACCCTGTTCTATTGCCCC	CGGAGGATAACAGGAGAGGC	240
PLC $\beta$ 3	AACTAGCCGCTCTCATTGGG	ACTGAGGGAGGAGCTAGTGG	176
PLC $\beta$ 4	GGAAGTGCCCTCTTTCTTGC	GCCTTCACTCTTCCACGTCA	130
PLC $\gamma$ 1	AGATCCGTGAAGTTGCCAG	TCAGCCTTGGTTCCGGAAA	193
PLC $\gamma$ 2	GATCATGGAGACTCGGCAGG	GACAACTGGGTGCCGTAGA	181
PLC $\delta$ 1	GCAAGATCATCGACCGCTC	CGTAGCTGTCATCCACCTGT	165
PLC $\delta$ 3	GACAGCAGCACCAAAAGGC	CGTGAGCGGATCTTGAGGAG	113
	CAGCAACTGACCCGAGTGTA	CTCAGGGTCAAAGGTGGTGT	222
PLC $\delta$ 4	TTCAATCCTGAGAGGCCAAT	TCCACTTTGGGGAGTTGTTG	86
PLC $\epsilon$	GGAGCCAACGTCTGTCTGAA	GAGTTTGGGAGCTGTGTGGA	118
PLC $\zeta$	AGACTTCTGCTTTTCGACA	TGTCGGTTCCTATCCTCTCG	137
PLC $\eta$ 1	CCGCAGAAAAGTCAGGCAAA	AGCTCCTCCACAGTCAGGT	171
	AGTAGGGCAGTGGGTTGAAG	TACACAACTCCGTGGCAGC	199
PLC $\eta$ 2	CGGCAGAGGGTGAAACAGAT	CTCGGCGGGTAGACATCATC	109
	TGTTTCATGTGGCTGTCAGTG	GACTTGGCTTCTGGCTTTTG	194

doi:10.1371/journal.pone.0123769.t001

collected with patch micropipettes to ensure the purity of the isolated ECs. ECs mRNA was extracted and purified (RNeasy Plus micro kit, Qiagen) before amplification using Message-BOOSTER Whole Transcriptome cDNA synthesis kit for qPCR (Epicentre Biotechnologies). Reverse transcription was performed using iScript kit (Bio-Rad) according to the manufacturer's instructions. The purity of the isolated ECs was further assessed by qPCR analysis of the relative abundance of endothelial specific (CD31) and SMCs specific (SM22) mRNA (CD31/SM22 ratio) in MAECs, PAECs and MCAECs (S1 Fig). qPCR was performed using a Stratagene MX3005 system using iTaq fast Syber Green with ROX (Bio-Rad) and are normalized to cyclophilin A expression.

## Immunocytochemistry

MA were cut longitudinally, and pinned (endothelium *en face*) on a Sylgard block. Arteries were fixed with 4% paraformaldehyde, permeabilized with 0.2% Triton X-100 then blocked with 4% normal donkey serum. Following overnight incubation at 4°C with primary antibodies (1:500; PLCβ3 Abcam #ab52199; PLCδ1 Abcam #ab154610; PLCγ2 Abcam #ab18983) in 0.1% Triton X-100, arteries were incubated for 1h with an Alexa Fluor 555-conjugated donkey anti-rabbit secondary antibody (Invitrogen). DAPI was applied to stain nuclei prior mounting for confocal imaging. Autofluorescence of the internal elastic lamina was also acquired. Fluorescence emissions were detected using a Zeiss LSM 510 confocal microscope (63X oil objective/1.4, ex: 405 nm, 488 nm and 543 nm). All images were deconvolved with Huygens professional software using experimentally determined point spread functions (PSFs) and reconstructed with Zen 2009 Light Edition.

## Western blotting

Protein extraction from MA was carried out by tissue immersion in ice-cooled acetone, 10% trichloroacetic acid and 10 mM dithiothreitol (DTT). Tissue was then lyophilized, disrupted and heated at 95°C for 10 minutes in SDS-gel sample buffer (60 mM Tris-HCl, pH 6.8, 2% SDS, 10% glycerol, 0.01% bromophenol blue, 0.1 M DTT) [24,25]. Finally, proteins were extracted by continuously mixing samples in SDS-gel sample buffer overnight at 4°C. Proteins were separated by SDS-PAGE on 7.5% acrylamide gels and transferred to nitrocellulose membranes (Bio-Rad). Membranes were blocked using 5% fat-free dry milk and then incubated with primary antibodies (1:1000; PLCβ3 Abcam #ab52199; PLCδ1 Abcam #ab154610; PLCγ2 Abcam #ab18983) for 1 hour at room temperature. Membranes were then washed and incubated with HRP-conjugated goat anti-rabbit secondary antibody (Jackson ImmunoResearch) for 1 hour at room temperature. Immunoreactive bands were revealed by enhanced chemiluminescence (Western Lightning Plus, PerkinElmer).

## Statistical analysis

Data are presented as means  $\pm$  SEM. One-way ANOVA with Turkey's multiple comparisons test was used to compare the means;  $P < 0.05$  was considered significant.

## Results

### mRNA expression of PLC isoforms

Expression of PLC isoforms was initially determined in freshly isolated arteries from 3 different vascular beds: MA, PA and MCA (Figs 1–4, panels A). While mRNA for 8 of the 13 PLC isoforms were detected in MA, 10 were found in MCA and 11 in PA. As shown in Fig 1A, PLCβ1, β3 and β4 mRNA was detected in all vascular beds studied. Interestingly, PLCβ2 was only

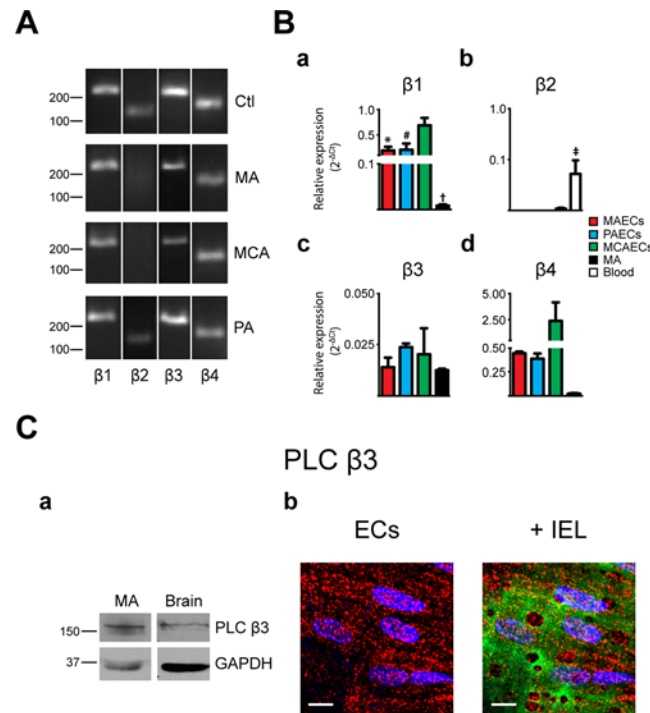


**Fig 1. Characterization of phospholipase C  $\beta$  isoforms in native arteries.** **A.** The presence of mRNA for phospholipase C (PLC)  $\beta$  isoforms was determined in mesenteric arteries (MA), pulmonary arteries (PA) and middle cerebral arteries (MCA) by PCR. Typical agarose gel electrophoresis of the PCR products showed the expression profile in different vascular beds. Brain and blood were used as positive control tissues.  $n = 3$ . **B.** Quantitative real time PCR analysis of mRNA expression levels of PLC $\beta$  isoforms in MA and freshly isolated endothelial cells (ECs) from MA, PA and MCA. Bar graphs show the expression profile of PLC $\beta$ 1 (a),  $\beta$ 2 (b),  $\beta$ 3 (c) and  $\beta$ 4 (d) isoforms in MAECs, PAECs, MCAECs, MA and blood as control for  $\beta$ 2.  $n = 3$ . \*  $P < 0.05$  between MAECs and MCAECs; #  $P < 0.05$  between PAECs and MCAECs; †  $P < 0.05$  between MCAECs and MAs; ‡  $P < 0.05$  between control tissue and MA. **C.** (a) Representative immunoblots of murine MA and brain that were obtained using the primary antibody anti-PLC  $\beta$ 3 (Abcam #ab52199). GAPDH was used as reference protein. Relevant molecular weight markers are indicated on the left.  $n = 3$ . (b) Intracellular distribution of PLC $\beta$ 3 immunoreactivity in ECs. (Left) Typical image showing labelling of PLC  $\beta$ 3 in red and nuclei in blue; scale = 10  $\mu$ m. (Right) Labelling of PLC  $\beta$ 3 (red) overlay with internal elastic lamina (IEL; green) where voids correspond to potential myoendothelial projections; nucleus in blue; scale = 10  $\mu$ m;  $n = 4$ .

doi:10.1371/journal.pone.0123769.g001

detected in PA. PLC $\gamma$  and  $\epsilon$  isoforms were expressed in all arteries tested (Figs 2A and 4A). While PLC $\delta$ 1 and  $\delta$ 3 were in all tested arteries, only MCA express  $\delta$ 4 (Fig 3A). PLC  $\zeta$  was only detected in testis, our positive control, with no noticeable expression in arteries (Fig 4A). The PLC $\eta$  family had a distinct expression pattern, as shown in Fig 4A. PLC $\eta$ 1 was found in MCA and PA but not in MA, whilst  $\eta$ 2 was detected only in PA. Data from PCR experiments are summarized in Table 2. However, these expression profiles represent mRNA from all cells found in the arterial wall, including both endothelium and vascular SMCs. Assessment of endothelial-specific PLC expression requires isolation of mRNA from preparations of ECs.

Endothelial PLC expression was quantified in freshly isolated MAECs, PAECs and MCAECs by qPCR. The purity of EC isolations was assessed by determining the expression ratio of EC vs. SMC markers (CD31 and SM22, respectively; S1 Fig) in both isolated arteries and corresponding EC preparations. This assessment confirmed that EC samples used were highly enriched in ECs. The relative expression of PLC isoforms in MAECs, PAECs and MCAECs as well as in MA was then determined (Figs 1–4, panels B). PCR and qPCR yielded

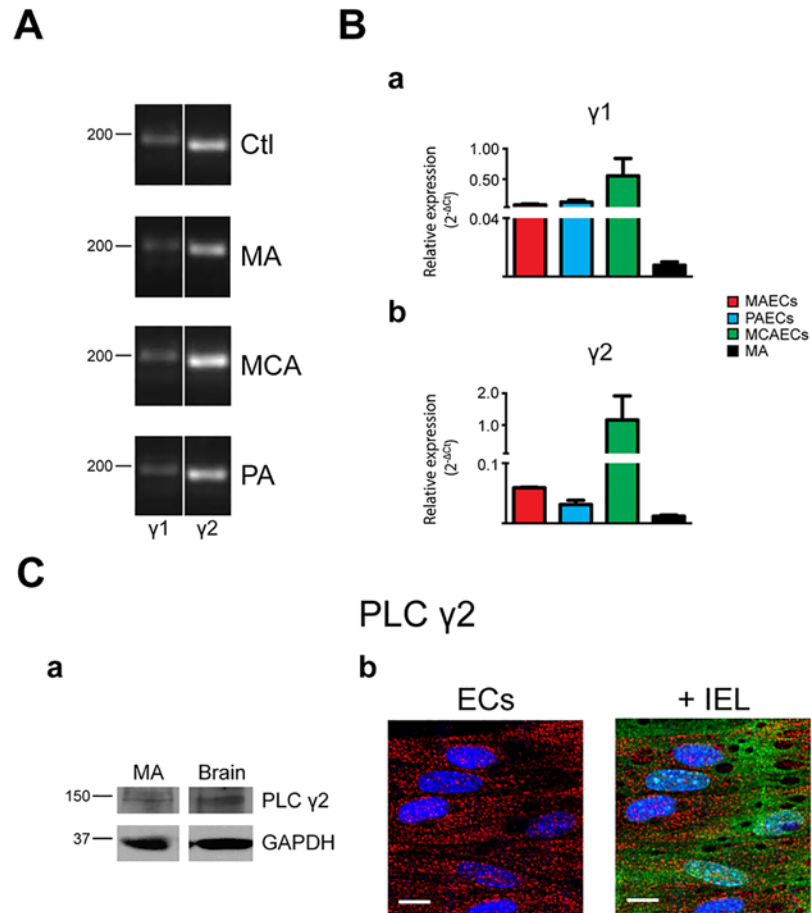


**Fig 2. Characterization of phospholipase C  $\gamma$  isoforms in native arteries.** **A.** The presence or mRNA for phospholipase C (PLC)  $\gamma$  isoforms was determined in mesenteric arteries (MA), pulmonary arteries (PA) and middle cerebral arteries (MCA) by PCR. Typical agarose gel electrophoresis of the PCR products showed the expression profile in the different vascular beds and brain was used as control tissue.  $n = 3$ . **B.** Quantitative real time PCR analysis of mRNA expression levels of PLC $\gamma$  isoforms in MA and freshly isolated endothelial cells (ECs) from MA, PA and MCA. Bar graphs show the expression profile of PLC $\gamma$ 1 (a) and  $\gamma$ 2 (b) isoforms in MAECs, PAECs, MCAECs and MA.  $n = 3$ . **C.** (a) Representative immunoblots of murine MA and brain that were analyzed using the primary antibody anti-PLC  $\gamma$ 2 (Abcam #ab18983). GAPDH was used as reference protein. Relevant molecular weight markers are indicated on the left.  $n = 3$ . (b) Intracellular distribution of PLC $\gamma$ 2 immunoreactivity in ECs. (Left) Typical image showing labelling of PLC $\gamma$ 2 in red and nuclei in blue; scale = 10  $\mu$ m. (Right) Labelling of PLC $\gamma$ 2 (red) overlay with internal elastic lamina (IEL; green) where voids correspond to potential myoendothelial projections; nucleus in blue; scale = 10  $\mu$ m;  $n = 4$ .

doi:10.1371/journal.pone.0123769.g002

similar expression profiles for PLC mRNA in MA with the exception of PLC $\beta$ 2 and  $\eta$ 1, which were only detected using the more sensitive qPCR. Therefore, mRNA encoding for nine PLC isoforms was detected in MA by qPCR. An almost identical PLC profile was observed in MAECs, with the exception that PLC $\eta$ 2 was undetectable in MAECs (Fig 4B). From a vascular bed point of view, slight differences were found between MAECs, PAECs and MCAECs. ECs from all arteries tested expressed at least 8 of the 13 PLC isoforms:  $\beta$ (1,3,4),  $\gamma$ (1–2),  $\delta$ (1,3) and  $\epsilon$ . Additionally, PAECs and MCAECs expressed PLC $\eta$ 1, whereas MAECs did not. In accordance with our findings in whole arterial preparations, PLC  $\delta$ 4 mRNA was only detected in MCAECs and PLC $\eta$ 2 was only detected in PAECs. These results are summarized in Table 2.

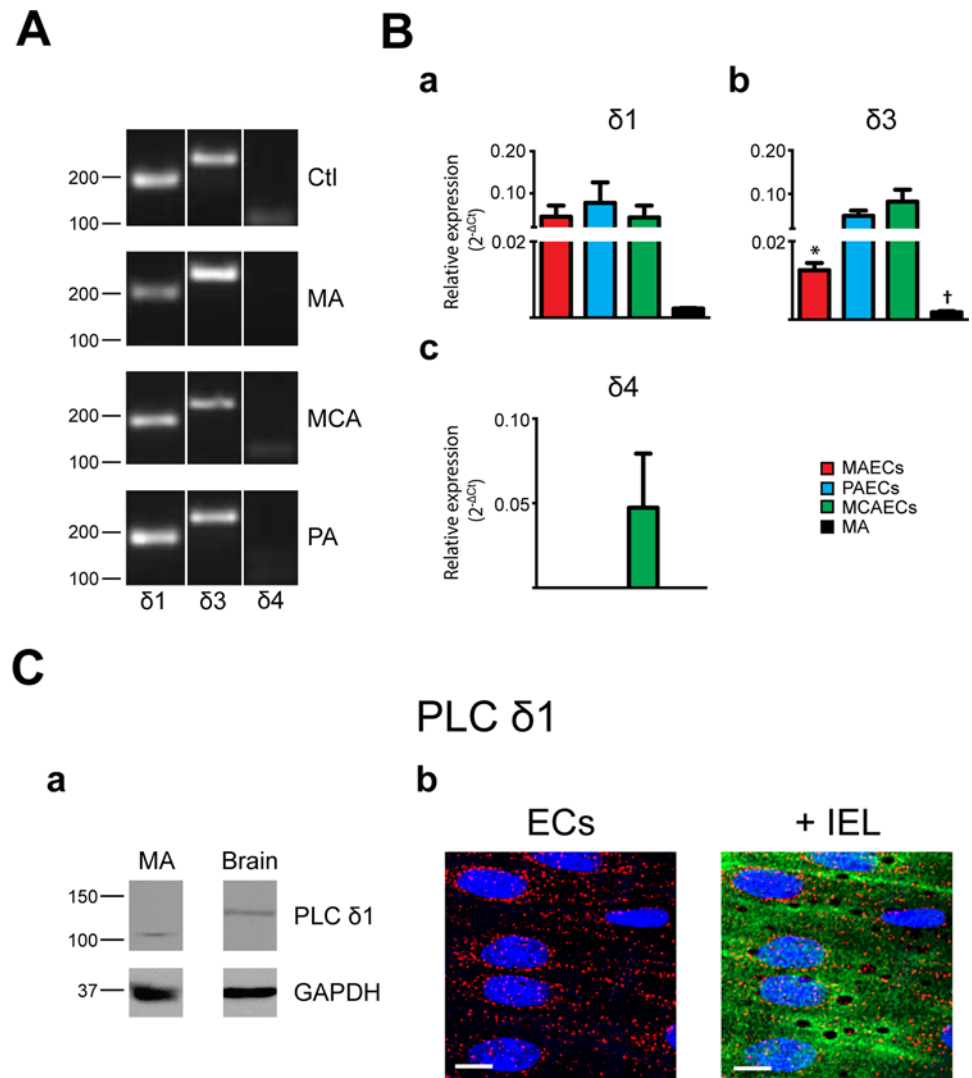


**Fig 3. Characterization of phospholipase C  $\delta$  isoforms in native arteries.** **A.** The presence of mRNA for phospholipase C (PLC)  $\delta$  isoforms was determined in mesenteric arteries (MA), pulmonary arteries (PA) and middle cerebral arteries (MCA) by PCR. Typical agarose gel electrophoresis of the PCR products showed the expression profile of PLC  $\delta$  isoforms in the different vascular beds and brain was used as control tissue.  $n = 3$ . **B.** Quantitative real time PCR analysis of mRNA expression levels of PLC  $\delta$  isoforms in MA and freshly isolated endothelial cells (ECs) from MA, PA and MCA. Bar graphs showed the expression profile of PLC  $\delta 1$  (a),  $\delta 3$  (b) and  $\delta 4$  (c) isoforms in MAECs, PAECs, MCAECs and MA.  $n = 3$ . \*  $P < 0.05$  between MAECs and MCAECs; †  $P < 0.05$  between MCAECs and MA. **C.** (a) Representative immunoblots of murine MA and brain that were analyzed using the primary antibody anti-PLC  $\delta 1$  (Abcam #ab154610). GAPDH was used as reference protein. Relevant molecular weight markers are indicated on the left.  $n = 3$ . (b) Intracellular distribution of PLC  $\delta 1$  immunoreactivity in ECs. (Left) Typical image showing labelling of PLC  $\delta 1$  in red and nuclei in blue; scale = 10  $\mu m$ . (Right) Labelling of PLC  $\delta 1$  (red) overlay with internal elastic lamina (IEL; green) where voids correspond to potential myoendothelial projections; nucleus in blue; scale = 10  $\mu m$ ;  $n = 4$ .

doi:10.1371/journal.pone.0123769.g003

### Protein expression of PLC isoforms

The three main PLC families are PLC $\beta$ , PLC $\gamma$  and PLC $\delta$  [26]. However, investigation of PLC isoform expression at the protein level was limited to the commercially available antibodies: PLC $\beta 3$ , PLC $\gamma 2$  and PLC $\delta 1$ . Western blotting was thus used to elucidate the expression of these

**Table 2. Summary of mRNA expression for phospholipase C isoforms.**

	qPCR				PCR		
	MAECs	PAECs	MCAECs	MA	MA	PA	MCA
PLCβ1	+	+	+	+	+	+	+
PLCβ2	-	-	-	-	-	+	-
PLCβ3	+	+	+	+	+	+	+
PLCβ4	+	+	+	+	+	+	+
PLCγ1	+	+	+	+	+	+	+
PLCγ2	+	+	+	+	+	+	+
PLCδ1	+	+	+	+	+	+	+
PLCδ3	+	+	+	+	+	+	+
PLCδ4	-	-	+	-	-	-	+
PLCε	+	+	+	+	+	+	+
PLCζ	-	-	-	-	-	-	-
PLCη1	-	+	+	+	-	+	+
PLCη2	-	+	-	-	-	+	-

MAECs, mesenteric arteries endothelial cells; PAECs, pulmonary arteries endothelial cells; MCAECs, middle cerebral arteries endothelial cells; MA, mesenteric arteries; PA, pulmonary arteries; MCA, middle cerebral arteries.

doi:10.1371/journal.pone.0123769.t002

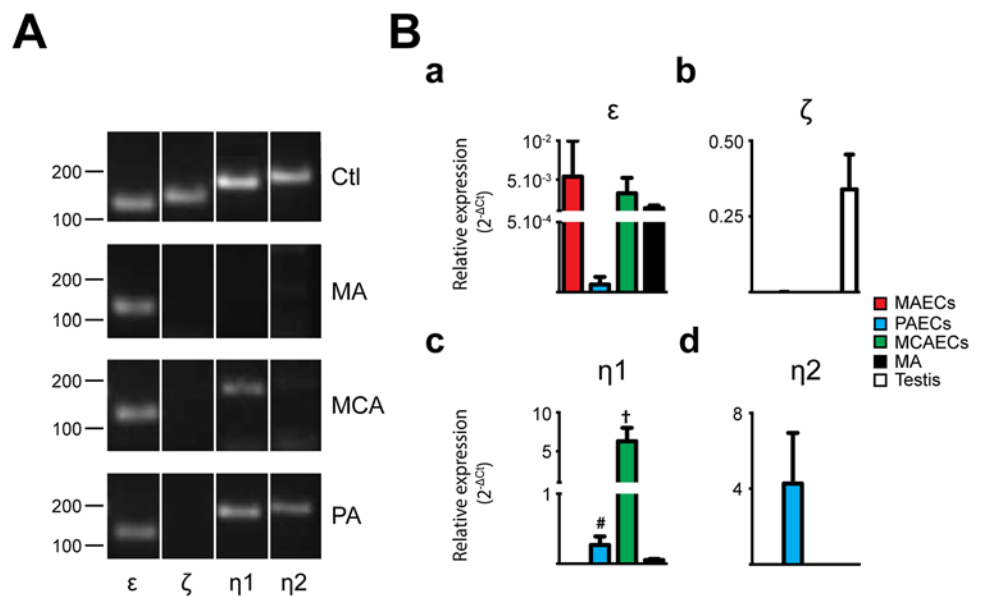


**Fig 4. Characterization of phospholipase C  $\epsilon$ ,  $\zeta$  and  $\eta$  isoforms in native arteries.** **A.** The presence of mRNA for phospholipase C (PLC)  $\epsilon$ ,  $\zeta$ ,  $\eta$ 1 and  $\eta$ 2 isoforms was determined in mesenteric arteries (MA), pulmonary arteries (PA) and middle cerebral arteries (MCA) by PCR. Typical agarose gel electrophoresis of the PCR products showed the expression profile of PLC $\epsilon$ ,  $\zeta$ ,  $\eta$ 1 and  $\eta$ 2 isoforms in the different vascular beds and brain or testis were used as control tissue.  $n = 3$ . **B.** Quantitative real time PCR analysis of mRNA expression levels of PLC $\epsilon$ ,  $\zeta$ ,  $\eta$ 1 and  $\eta$ 2 isoforms in MA and freshly isolated endothelial cells (ECs) from MA, PA and MCA. Bar graphs show the expression of PLC $\epsilon$  (a),  $\zeta$  (b),  $\eta$ 1 (c) and  $\eta$ 2 (d) isoforms in MAECs, PAECs, MCAECs, MA and testis as positive control for  $\zeta$ .  $n = 3$ . \*  $P < 0.05$  between MAECs and MCAECs; #  $P < 0.05$  between PAECs and MCAECs; †  $P < 0.05$  between MCAECs and MA.

doi:10.1371/journal.pone.0123769.g004

PLC isoforms in MA at the protein level. As shown in [Fig 1Ca](#), PLC $\beta$ 3 antibodies revealed a band of 150-kDa in MA extracts. PLC $\delta$ 1 and PLC $\gamma$ 2 antibodies revealed bands of 100-kDa and 150-kDa, respectively ([Figs 2Ca](#) and [3Ca](#)).

### Subcellular distribution of PLC isoforms

Since PLC $\beta$ 3,  $\gamma$ 2 and  $\delta$ 1 were detected in MA by western blotting, we next determined their respective presence and subcellular distribution. Immunofluorescence experiments were performed on MA sections dissected and immobilized with the endothelium in an *en face* configuration. All isoforms displayed a similar intracellular distribution. PLC $\beta$ 3 ([Fig 1Cb](#)),  $\gamma$ 2 ([Fig 2Cb](#)) and  $\delta$ 1 ([Fig 3Cb](#)) were homogeneously distributed in intact endothelium of MA.

### Discussion

PLCs are crucial components of the phosphoinositide signalling pathway through their hydrolysis of PIP<sub>2</sub> into IP<sub>3</sub> and 1,2-DAG. The 13 mammalian PLC isozymes identified so far are organized within 6 families:  $\beta$ (1–4),  $\gamma$ (1–2),  $\delta$ (1,3,4),  $\epsilon$ ,  $\zeta$  and  $\eta$ (1–2) [5]. PLC isoforms are distinct in their activation mode, expression levels, catalytic regulation, cellular localization and tissue distribution. PLC $\beta$  and  $\gamma$  are considered as “first line PLCs” as they are activated by extracellular stimuli. In contrast, PLC $\delta$ ,  $\epsilon$ ,  $\eta$  and  $\zeta$  are secondary PLCs, being activated by intracellular Ca<sup>2+</sup> [27]. For example, PLC $\gamma$  isoforms are activated by tyrosine kinase receptors while members of the PLC $\beta$  family are activated by G protein-coupled receptors [28,29]. These distinct characteristics allow PLC activity to be involved in a wide range of functions in both physiology and pathophysiology [30]. For example, each neuronal PLC isoform selectively couples with a specific neurotransmitter and contributes to distinct functions. PLC $\beta$ 1 knockout mice are afflicted with epilepsy while abnormal activity and expression level of PLC $\gamma$ 1 are detected in pathologies including Huntington's disease, depression and Alzheimer's disease [7,31]. These numerous pathophysiological roles illustrate the extensive variety of cellular functions associated with each individual PLC isoform. Despite their crucial role in cellular signalling, the expression pattern of PLC isozymes remains to be established in native ECs. This study is the first study of PLC isoform expression at the mRNA level in murine resistance arteries from 3 distinct vascular beds: MA, PA and MCA. We also examined PLC expression pattern in freshly isolated ECs from these arterial beds. Finally, we demonstrated the presence of immunoreactivity for 3 major PLC isoforms ( $\beta$ 3,  $\gamma$ 2 and  $\delta$ 1) in MA and their homogenous subcellular distribution in MA endothelium.

Recently, Lo Vasco and coll. Report that of 10 out of 13 PLC isoforms are expressed in HUVECs, a cultured ECs model [18]. Interestingly, our data slightly differs from that of Lo Vasco *et al.*: PLC $\beta$ 1 and  $\epsilon$  are expressed in native ECs from all vascular beds tested but not in HUVECs. However,  $\beta$ 2 is absent from freshly isolated murine ECs but is expressed in HUVECs. Also,  $\eta$ 1 and  $\eta$ 2 are expressed in HUVECs but were not detected in the 3 types of native ECs. These discrepancies might be explained by the alteration of endothelial phenotype maintained in culture [32]. In vitro, ECs lose their MEP, an essential architecture for the communication with vascular SMCs. Therefore, in addition to passaging, culture media and the absence of shear stress, the loss of cellular polarity may contribute to the observed differences in PLC expression in native and cultured ECs. Moreover, while we used arterial tissues in the present study, Lo Vasco and coll. used cells from veins. Hence, arteries to veins differences may also explain the different expression reported.

Employing qPCR allowed us to identify the PLC isoforms expressed specifically in freshly isolated ECs from MA, PA and MCA. Three of the four known PLC $\beta$  isoforms were detected in all ECs tested: PLC $\beta$ 1,  $\beta$ 3 and  $\beta$ 4. Moreover, PLC $\beta$ 3 expression was also found at the protein

level with immunoblots and confocal imaging. This is an interesting finding since PLC  $\beta$ 3 is involved in the VEGF-dependent inhibition of vascular permeability [33]. However, the roles of endothelial  $\beta$ 1 and  $\beta$ 4 remain to be determined. Undetectable expression of PLC  $\beta$ 2 from ECs was anticipated considering its involvement in platelets and hematopoietic cells chemotaxis [5,34–36]. Both PLC $\gamma$  isoforms were detected in native ECs. PLC $\gamma$ 1 appears to be required for normal development as knockout mice do not survive beyond E9, due to a generalized growth failure attributed to the loss of both erythroid progenitors cells and ECs necessary for erythropoiesis and vasculogenesis [37,38]. On the other hand, PLC $\gamma$ 2 appears to be selectively expressed in blood cells, spleen and thymus [39]. The present study is the first report of PLC $\gamma$ 2 expression in native ECs. Detection of PLC $\gamma$ 2 expression by qPCR was further supported by immunoblotting. Moreover, immunostaining showed a homogeneous endothelial distribution of the enzyme. Obviously, the specific role of PLC $\gamma$ 2 in ECs is yet to be elucidated. Consistent with reports of PLC $\delta$  subtypes being expressed in porcine aortic ECs [40], we detected all three PLC $\delta$  isoforms in MCAECs whilst PLC $\delta$ 4 was absent from MAECs and PAECs. PLC $\delta$  isoforms are among the most sensitive to  $\text{Ca}^{2+}$ , suggesting a potential role downstream of changes in endothelial  $\text{Ca}^{2+}$  dynamics [41,42]. However, elucidating the role of PLC $\delta$ 4 specific function in MCAECs will require additional investigation. Studies employing a PLC $\delta$ 4-null mouse have shown PLC $\delta$ 4 to be involved in the initial stages of fertilization [6] but its role in endothelial function remains to be established. Immunoblotting of PLC  $\delta$ 1 revealed differences in apparent molecular weight in MA and brain. This can be explained by various types of post-translational modification, such as multiple phosphorylations as described by Fujii *et al.* [43]. Finally, we detected PLC $\epsilon$ , but not PLC $\zeta$ , in freshly isolated ECs from all vascular beds. In contrast, while PLC $\eta$ 2 is only expressed in PAECs, PLC $\eta$ 1 was not detected in MAECs. Similar to  $\delta$ 4, there is currently no information available regarding the expression or function of PLC $\epsilon$ ,  $\zeta$ ,  $\eta$ 1 and  $\eta$ 2 in ECs. However, the function of these PLC isoforms has been examined in other cell types. For example, PLC $\epsilon$ -null mice show abnormal development of the aortic and pulmonary valves [9], while PLC $\zeta$  expression/function was reported as sperm-specific [44] and PLC $\eta$ 1 and  $\eta$ 2 seem to be involved in neural system regulation [5]. In summary, very little is known about the function of PLC isoforms in ECs, and further studies are therefore required to investigate their respective and specific roles.

ECs are heterogeneous both in structure and function across the vascular tree under normal or pathological conditions [20,21]. For example, rat PAECs have a broader and shorter shape than rat aortic ECs [45]. ECs are involved in several physiological functions, the relative importance of which varies according to blood vessel type (conduit *vs.* resistance) or vascular bed, including vascular permeability, hemostasis or vasomotor tone in response to the specific requirements of the perfused organ. For example, pulmonary vasculature is exposed to a low-pressure, high flow of oxygen-deprived blood. Therefore, the proteins expressed in ECs will have varied in order to adapt to the needs of their particular vascular bed of origin [19]. We determined the expression of all known mammalian PLC isoforms in native ECs of resistance arteries from three different vascular beds (MA, PA and MCA) by qPCR and observed a similar pattern of expression in each case. For 10 isoforms, the pattern of expression was constant between the 3 vascular beds (8 isoforms detected while 2 other were not detected). However, we observed slight differences for 3 isoforms: PLC $\delta$ 4 and  $\eta$ 2 were detected exclusively in MCAECs and PAECs, respectively, whereas PLC $\eta$ 1 was expressed in MCAECs and PAECs but not MAECs.

Endothelial PLC might be involved in the modulation of  $\text{Ca}^{2+}$  dependant vasoregulatory signals. In fact, the release of  $\text{Ca}^{2+}$  through  $\text{IP}_3$  receptors in the ER membrane is stimulated by the  $\text{IP}_3$  generated upon activation of membrane receptors leading to activation of PLC. PLC are known to regulate  $\text{Ca}^{2+}$  levels and thus might be involved in the modulation of intracellular  $\text{Ca}^{2+}$  dynamics. In 2013, De Bock and coll. reviewed the signalling pathways

including PLCs pathway leading to intracellular  $\text{Ca}^{2+}$  elevation in blood-brain-barrier ECs [46]. Although all PLCs are  $\text{Ca}^{2+}$ -dependent, they vary with respect to their sensitivity to  $\text{Ca}^{2+}$ . PLC $\delta$  and  $\eta$  are the most sensitive to  $\text{Ca}^{2+}$  and are involved in potentiating  $\text{Ca}^{2+}$  signalling [47,48]. In a recent study, PLC $\beta$ 1 and  $\beta$ 4 were shown to be involved in distinct histamine-induced  $\text{Ca}^{2+}$  oscillations [49].

In ECs, increased  $\text{IP}_3$  production results in the release of  $\text{Ca}^{2+}$  from intracellular stores [50] and the  $\text{IP}_3\text{R}$  is the only ER  $\text{Ca}^{2+}$  channels expressed in these cells [51].  $\text{IP}_3$  is generated through activation of G protein-coupled receptors or tyrosine kinase receptors which activate PLC $\beta$  and  $\gamma$  respectively [52]. Multiple cellular functions are regulated by changes in intracellular  $\text{Ca}^{2+}$ . Therefore, specificity of the  $\text{Ca}^{2+}$  signal is often achieved through spatial and temporal compartmentalization of  $\text{Ca}^{2+}$  signals. Several different patterns of  $\text{Ca}^{2+}$  dynamics have recently been described in ECs:  $\text{Ca}^{2+}$  pulsars, TRPV4- and TRPA1-sparklets or wavelets, each generated by a specific pathway [11,12,14,53].  $\text{Ca}^{2+}$  pulsars are MEP localized signals consisting of a spontaneous  $\text{Ca}^{2+}$  release from  $\text{IP}_3$  receptors [11]. Limited information is currently available on the regulatory mechanisms of  $\text{Ca}^{2+}$  pulsars. However, specific PLC activation could be responsible for localized  $\text{Ca}^{2+}$  signalling such as  $\text{Ca}^{2+}$  pulsars. Cytoplasmic gradients of  $\text{IP}_3$  would result in a limited activation of  $\text{IP}_3\text{R}$  and restricted propagation of the signal. Although our immunocytochemistry data showed a homogeneous distribution of PLC $\beta$ 3,  $\gamma$ 2 and  $\delta$ 1 in ECs, PLC partners and modulators could be heterogeneously distributed within the cell. Microdomains would then result from these associations as well as the distribution of proteins involved in  $\text{Ca}^{2+}$  sequestration. For example, Gonzales and coll. have recently shown colocalization of PLC $\gamma$ 1 with  $\text{IP}_3\text{R}$ , TRPM4 and TRPC6 in VSMC from cerebral arteries and elegantly demonstrated its requirement for pressure-induced membrane depolarization and myogenic vasoconstriction [13]. Moreover, TRPV4 channels responsible for  $\text{Ca}^{2+}$  sparklets are clustered in EC microdomains at MEP where they are modulated by PLC isoforms [54,55]. As for TRP channels, specific PLC isoforms can be localized in microdomains to have a pivotal role in the modulation of  $\text{Ca}^{2+}$  pulsars [56]. Moreover, our investigation of the subcellular localization of PLC was limited to three isoforms due to a lack of commercially available, reliable antibodies for the other isoforms. Therefore, the subcellular distribution of other members of the PLC family in native endothelium remains to be determined.

In summary, in this study we established for the PLCs that are expressed in native endothelium and freshly isolated ECs. We showed that 8 out of the 13 mammalian PLC isoforms are expressed in MAECs and 10 in PAECs and MCAECs. These results represent an important step forward in our understanding of the intracellular signalling pathways and their role in the regulation of endothelial microdomains. Further investigation of the subcellular distribution and biological function of these PLC isoforms is required in order to have a better understanding of their relative involvement in regulating endothelial function.

## Supporting Information

**S1 Fig. Purity of freshly isolated endothelial cells samples.** Quantitative real time PCR analysis of mRNA expression levels of CD31, an endothelial-specific marker, and SM22, a smooth muscle cell-specific marker. (A) Pie chart illustrating the relative expression of CD31 to SM22 (CD31/SM22 ratio) in mesenteric arteries (MA) and in endothelial cells isolated from mesenteric arteries (MAECs). (B) Pie chart illustrating CD31/SM22 ratio in pulmonary arteries (PA) and in endothelial cells from pulmonary arteries (PAECs). (C) Pie chart illustrating CD31/SM22 in middle cerebral arteries (MCA) and in endothelial cells from middle cerebral arteries (MCAECs).  $n = 3$ . (TIF)

## Acknowledgments

The authors are grateful to Maya Mamarbachi and Louis R. Villeneuve for their helpful assistance in molecular biology and confocal microscopy. The authors are also thankful to Dr. Bruce G. Allen for his greatly appreciated critical editing of the manuscript.

## Author Contributions

Conceived and designed the experiments: DMB JL. Performed the experiments: DMB FT AB. Analyzed the data: DMB FT. Contributed reagents/materials/analysis tools: DMB FT NRD CC JCT. Wrote the paper: DMB JCT JD JL.

## References

1. Berridge MJ, Irvine RF. Inositol trisphosphate, a novel second messenger in cellular signal transduction. *Nature*. 1984; 312: 315–321. PMID: [6095092](#)
2. Nishizuka Y. The molecular heterogeneity of protein kinase C and its implications for cellular regulation. *Nature*. 1988; 334: 661–665. PMID: [3045562](#)
3. Kishimoto A, Takai Y, Mori T, Kikkawa U, Nishizuka Y. Activation of calcium and phospholipid-dependent protein kinase by diacylglycerol, its possible relation to phosphatidylinositol turnover. *J Biol Chem*. 1980; 255: 2273–2276. PMID: [7358670](#)
4. Rohacs T. Phosphoinositide regulation of non-canonical transient receptor potential channels. *Cell Calcium*. 2009; 45: 554–565. doi: [10.1016/j.ceca.2009.03.011](#) PMID: [19376575](#)
5. Suh PG, Park JI, Manzoli L, Cocco L, Peak JC, Katan M, et al. Multiple roles of phosphoinositide-specific phospholipase C isozymes. *BMB Rep*. 2008; 41: 415–434. PMID: [18593525](#)
6. Fukami K, Nakao K, Inoue T, Kataoka Y, Kurokawa M, Fissore RA, et al. Requirement of phospholipase Cdelta4 for the zona pellucida-induced acrosome reaction. *Science*. 2001; 292: 920–923. PMID: [11340203](#)
7. Kim D, Jun KS, Lee SB, Kang NG, Min DS, Kim YH, et al. Phospholipase C isozymes selectively couple to specific neurotransmitter receptors. *Nature*. 1997; 389: 290–293. PMID: [9305844](#)
8. Li Z, Jiang H, Xie W, Zhang Z, Smrcka AV, Wu D. Roles of PLC-beta2 and -beta3 and PI3Kgamma in chemoattractant-mediated signal transduction. *Science*. 2000; 287: 1046–1049. PMID: [10669417](#)
9. Tadano M, Edamatsu H, Minamisawa S, Yokoyama U, Ishikawa Y, Suzuki N, et al. Congenital semilunar valvulogenesis defect in mice deficient in phospholipase C epsilon. *Mol Cell Biol*. 2005; 25: 2191–2199. PMID: [15743817](#)
10. Jiang H, Kuang Y, Wu Y, Xie W, Simon MI, Wu D. Roles of phospholipase C beta2 in chemoattractant-elicited responses. *Proc Natl Acad Sci U S A*. 1997; 94: 7971–7975. PMID: [9223297](#)
11. Ledoux J, Taylor MS, Bonev AD, Hannah RM, Solodushko V, Shui B, et al. Functional architecture of inositol 1,4,5-trisphosphate signaling in restricted spaces of myoendothelial projections. *Proc Natl Acad Sci U S A*. 2008; 105: 9627–9632. doi: [10.1073/pnas.0801963105](#) PMID: [18621682](#)
12. Sonkusare SK, Bonev AD, Ledoux J, Liedtke W, Kotlikoff MI, Heppner TJ, et al. Elementary Ca<sup>2+</sup> signals through endothelial TRPV4 channels regulate vascular function. *Science*. 2012; 336: 597–601. doi: [10.1126/science.1216283](#) PMID: [22556255](#)
13. Gonzales AL, Yang Y, Sullivan MN, Sanders L, Dabertrand F, Hill-Eubanks DC, et al. A PLCgamma1-dependent, force-sensitive signaling network in the myogenic constriction of cerebral arteries. *Sci Signal*. 2014; 7: ra49. doi: [10.1126/scisignal.2004732](#) PMID: [24866019](#)
14. Sullivan MN, Gonzales AL, Pires PW, Bruhl A, Leo MD, Li W, et al. Localized TRPA1 channel Ca<sup>2+</sup> signals stimulated by reactive oxygen species promote cerebral artery dilation. *Sci Signal*. 2015; 8: ra2. doi: [10.1126/scisignal.2005659](#) PMID: [25564678](#)
15. Bhattacharya R, Kwon J, Li X, Wang E, Patra S, Bida JP, et al. Distinct role of PLCbeta3 in VEGF-mediated directional migration and vascular sprouting. *J Cell Sci*. 2009; 122: 1025–1034. doi: [10.1242/jcs.041913](#) PMID: [19295129](#)
16. Lawson ND, Mugford JW, Diamond BA, Weinstein BM. phospholipase C gamma-1 is required downstream of vascular endothelial growth factor during arterial development. *Genes Dev*. 2003; 17: 1346–1351. PMID: [12782653](#)
17. Crijen V, Visnjic D, Banfic H. Presence of different phospholipase C isoforms in the nucleus and their activation during compensatory liver growth. *FEBS Lett*. 2004; 571: 35–42. PMID: [15280014](#)

18. Lo Vasco VR, Pacini L, Di Raimo T, D'Arcangelo D, Businaro R. Expression of phosphoinositide-specific phospholipase C isoforms in human umbilical vein endothelial cells. *J Clin Pathol*. 2011; 64: 911–915. doi: [10.1136/jclinpath-2011-200096](https://doi.org/10.1136/jclinpath-2011-200096) PMID: [21742750](https://pubmed.ncbi.nlm.nih.gov/21742750/)
19. Cines DB, Pollak ES, Buck CA, Loscalzo J, Zimmerman GA, McEver RP, et al. Endothelial cells in physiology and in the pathophysiology of vascular disorders. *Blood*. 1998; 91: 3527–3561. PMID: [9572988](https://pubmed.ncbi.nlm.nih.gov/9572988/)
20. Aird WC. Phenotypic heterogeneity of the endothelium: I. Structure, function, and mechanisms. *Circ Res*. 2007; 100: 158–173. PMID: [17272818](https://pubmed.ncbi.nlm.nih.gov/17272818/)
21. Aird WC. Phenotypic heterogeneity of the endothelium: II. Representative vascular beds. *Circ Res*. 2007; 100: 174–190. PMID: [17272819](https://pubmed.ncbi.nlm.nih.gov/17272819/)
22. Kirby BS, Bruhl A, Sullivan MN, Francis M, Dinunno FA, Earley S. Robust internal elastic lamina fenestration in skeletal muscle arteries. *PLoS One*. 2013; 8: e54849. doi: [10.1371/journal.pone.0054849](https://doi.org/10.1371/journal.pone.0054849) PMID: [23359815](https://pubmed.ncbi.nlm.nih.gov/23359815/)
23. Socha MJ, Hakim CH, Jackson WF, Segal SS. Temperature effects on morphological integrity and Ca<sup>2+</sup>(+) signaling in freshly isolated murine feed artery endothelial cell tubes. *Am J Physiol Heart Circ Physiol*. 2011; 301: H773–783. doi: [10.1152/ajpheart.00214.2011](https://doi.org/10.1152/ajpheart.00214.2011) PMID: [21705671](https://pubmed.ncbi.nlm.nih.gov/21705671/)
24. Johnson RP, El-Yazbi AF, Takeya K, Walsh EJ, Walsh MP, Cole WC. Ca<sup>2+</sup> sensitization via phosphorylation of myosin phosphatase targeting subunit at threonine-855 by Rho kinase contributes to the arterial myogenic response. *J Physiol*. 2009; 587: 2537–2553. doi: [10.1113/jphysiol.2008.168252](https://doi.org/10.1113/jphysiol.2008.168252) PMID: [19359365](https://pubmed.ncbi.nlm.nih.gov/19359365/)
25. Takeya K, Loutzenhiser K, Shiraishi M, Loutzenhiser R, Walsh MP. A highly sensitive technique to measure myosin regulatory light chain phosphorylation: the first quantification in renal arterioles. *Am J Physiol Renal Physiol*. 2008; 294: F1487–1492. doi: [10.1152/ajprenal.00060.2008](https://doi.org/10.1152/ajprenal.00060.2008) PMID: [18400874](https://pubmed.ncbi.nlm.nih.gov/18400874/)
26. Kadamur G, Ross EM. Mammalian phospholipase C. *Annu Rev Physiol*. 2013; 75: 127–154. doi: [10.1146/annurev-physiol-030212-183750](https://doi.org/10.1146/annurev-physiol-030212-183750) PMID: [23140367](https://pubmed.ncbi.nlm.nih.gov/23140367/)
27. Yang YR, Follo MY, Cocco L, Suh PG. The physiological roles of primary phospholipase C. *Adv Biol Regul*. 2013; 53: 232–241. doi: [10.1016/j.jbior.2013.08.003](https://doi.org/10.1016/j.jbior.2013.08.003) PMID: [24041464](https://pubmed.ncbi.nlm.nih.gov/24041464/)
28. Smrcka AV, Sternweis PC. Regulation of purified subtypes of phosphatidylinositol-specific phospholipase C beta by G protein alpha and beta gamma subunits. *J Biol Chem*. 1993; 268: 9667–9674. PMID: [8387502](https://pubmed.ncbi.nlm.nih.gov/8387502/)
29. Kim HK, Kim JW, Zilberstein A, Margolis B, Kim JG, Schlessinger J, et al. PDGF stimulation of inositol phospholipid hydrolysis requires PLC-gamma 1 phosphorylation on tyrosine residues 783 and 1254. *Cell*. 1991; 65: 435–441. PMID: [1708307](https://pubmed.ncbi.nlm.nih.gov/1708307/)
30. Gresset A, Sondek J, Harden TK. The phospholipase C isozymes and their regulation. *Subcell Biochem*. 2012; 58: 61–94. doi: [10.1007/978-94-007-3012-0\\_3](https://doi.org/10.1007/978-94-007-3012-0_3) PMID: [22403074](https://pubmed.ncbi.nlm.nih.gov/22403074/)
31. Jang HJ, Yang YR, Kim JK, Choi JH, Seo YK, Lee YH, et al. Phospholipase C-gamma1 involved in brain disorders. *Adv Biol Regul*. 2013; 53: 51–62. doi: [10.1016/j.jbior.2012.09.008](https://doi.org/10.1016/j.jbior.2012.09.008) PMID: [23063587](https://pubmed.ncbi.nlm.nih.gov/23063587/)
32. Grant DS, Tashiro K, Segui-Real B, Yamada Y, Martin GR, Kleinman HK. Two different laminin domains mediate the differentiation of human endothelial cells into capillary-like structures in vitro. *Cell*. 1989; 58: 933–943. PMID: [2528412](https://pubmed.ncbi.nlm.nih.gov/2528412/)
33. Hoepfner LH, Phoenix KN, Clark KJ, Bhattacharya R, Gong X, Sciuto TE, et al. Revealing the role of phospholipase Cbeta3 in the regulation of VEGF-induced vascular permeability. *Blood*. 2012; 120: 2167–2173. doi: [10.1182/blood-2012-03-417824](https://doi.org/10.1182/blood-2012-03-417824) PMID: [22674805](https://pubmed.ncbi.nlm.nih.gov/22674805/)
34. Mao GF, Kunapuli SP, Koneti Rao A. Evidence for two alternatively spliced forms of phospholipase C-beta2 in haematopoietic cells. *Br J Haematol*. 2000; 110: 402–408. PMID: [10971398](https://pubmed.ncbi.nlm.nih.gov/10971398/)
35. Sun L, Mao G, Kunapuli SP, Dhanasekaran DN, Rao AK. Alternative splice variants of phospholipase C-beta2 are expressed in platelets: effect on Galphaq-dependent activation and localization. *Platelets*. 2007; 18: 217–223. PMID: [17497434](https://pubmed.ncbi.nlm.nih.gov/17497434/)
36. Tang W, Zhang Y, Xu W, Harden TK, Sondek J, Sun L, et al. A PLCbeta/PI3Kgamma-GSK3 signaling pathway regulates cofilin phosphatase slingshot2 and neutrophil polarization and chemotaxis. *Dev Cell*. 2011; 21: 1038–1050. doi: [10.1016/j.devcel.2011.10.023](https://doi.org/10.1016/j.devcel.2011.10.023) PMID: [22172670](https://pubmed.ncbi.nlm.nih.gov/22172670/)
37. Ji QS, Winnier GE, Niswender KD, Horstman D, Wisdom R, Magnuson MA, et al. Essential role of the tyrosine kinase substrate phospholipase C-gamma1 in mammalian growth and development. *Proc Natl Acad Sci U S A*. 1997; 94: 2999–3003. PMID: [9096335](https://pubmed.ncbi.nlm.nih.gov/9096335/)
38. Liao HJ, Kume T, McKay C, Xu MJ, Ihle JN, Carpenter G. Absence of erythropoiesis and vasculogenesis in Plcg1-deficient mice. *J Biol Chem*. 2002; 277: 9335–9341. PMID: [11744703](https://pubmed.ncbi.nlm.nih.gov/11744703/)
39. Homma Y, Takenawa T, Emori Y, Sorimachi H, Suzuki K. Tissue- and cell type-specific expression of mRNAs for four types of inositol phospholipid-specific phospholipase C. *Biochem Biophys Res Commun*. 1989; 164: 406–412. PMID: [2553017](https://pubmed.ncbi.nlm.nih.gov/2553017/)

40. Fu Y, Cheng JX, Hong SL. Characterization of cytosolic phospholipases C from porcine aortic endothelial cells. *Thromb Res*. 1994; 73: 405–417. PMID: [8073393](#)
41. Allen V, Swigart P, Cheung R, Cockcroft S, Katan M. Regulation of inositol lipid-specific phospholipase cdelta by changes in Ca<sup>2+</sup> ion concentrations. *Biochem J*. 1997; 327 (Pt 2): 545–552. PMID: [9359428](#)
42. Kim YH, Park TJ, Lee YH, Baek KJ, Suh PG, Ryu SH, et al. Phospholipase C-delta1 is activated by capacitative calcium entry that follows phospholipase C-beta activation upon bradykinin stimulation. *J Biol Chem*. 1999; 274: 26127–26134. PMID: [10473563](#)
43. Fujii M, Yi KS, Kim MJ, Ha SH, Ryu SH, Suh PG, et al. Phosphorylation of phospholipase C-delta 1 regulates its enzymatic activity. *J Cell Biochem*. 2009; 108: 638–650. doi: [10.1002/jcb.22297](#) PMID: [19681039](#)
44. Saunders CM, Larman MG, Parrington J, Cox LJ, Royse J, Blayney LM, et al. PLC zeta: a sperm-specific trigger of Ca(2+) oscillations in eggs and embryo development. *Development*. 2002; 129: 3533–3544. PMID: [12117804](#)
45. Kibria G, Heath D, Smith P, Biggar R. Pulmonary endothelial pavement patterns. *Thorax*. 1980; 35: 186–191. PMID: [7385090](#)
46. De Bock M, Wang N, Decrock E, Bol M, Gadicherla AK, Culot M, et al. Endothelial calcium dynamics, connexin channels and blood-brain barrier function. *Prog Neurobiol*. 2013; 108: 1–20. doi: [10.1016/j.pneurobio.2013.06.001](#) PMID: [23851106](#)
47. Rebecchi MJ, Pentylala SN. Structure, function, and control of phosphoinositide-specific phospholipase C. *Physiol Rev*. 2000; 80: 1291–1335. PMID: [11015615](#)
48. Vines CM. Phospholipase C. *Adv Exp Med Biol*. 2012; 740: 235–254. doi: [10.1007/978-94-007-2888-2\\_10](#) PMID: [22453945](#)
49. Ishida S, Matsu-Ura T, Fukami K, Michikawa T, Mikoshiba K. Phospholipase C-beta1 and beta4 contribute to non-genetic cell-to-cell variability in histamine-induced calcium signals in HeLa cells. *PLoS One*. 2014; 9: e86410. doi: [10.1371/journal.pone.0086410](#) PMID: [24475116](#)
50. Clapham DE. Calcium signaling. *Cell*. 1995; 80: 259–268. PMID: [7834745](#)
51. Ledoux J, Bonev AD, Nelson MT. Ca<sup>2+</sup>-activated K<sup>+</sup> channels in murine endothelial cells: block by intracellular calcium and magnesium. *J Gen Physiol*. 2008; 131: 125–135. doi: [10.1085/jgp.200709875](#) PMID: [18195387](#)
52. Carafoli E, Santella L, Branca D, Brini M. Generation, control, and processing of cellular calcium signals. *Crit Rev Biochem Mol Biol*. 2001; 36: 107–260. PMID: [11370791](#)
53. Tran CH, Taylor MS, Plane F, Nagaraja S, Tsoukias NM, Solodushko V, et al. Endothelial Ca<sup>2+</sup> wavelets and the induction of myoendothelial feedback. *Am J Physiol Cell Physiol*. 2012; 302: C1226–1242. doi: [10.1152/ajpcell.00418.2011](#) PMID: [22277756](#)
54. Garcia-Elias A, Mrkonjic S, Pardo-Pastor C, Inada H, Hellmich UA, Rubio-Moscardo F, et al. Phosphatidylinositol-4,5-bisphosphate-dependent rearrangement of TRPV4 cytosolic tails enables channel activation by physiological stimuli. *Proc Natl Acad Sci U S A*. 2013; 110: 9553–9558. doi: [10.1073/pnas.1220231110](#) PMID: [23690576](#)
55. Sonkusare SK, Dalsgaard T, Bonev AD, Hill-Eubanks DC, Kotlikoff MI, Scott JD, et al. AKAP150-dependent cooperative TRPV4 channel gating is central to endothelium-dependent vasodilation and is disrupted in hypertension. *Sci Signal*. 2014; 7: ra66. doi: [10.1126/scisignal.2005052](#) PMID: [25005230](#)
56. Dunn KM, Hill-Eubanks DC, Liedtke WB, Nelson MT. TRPV4 channels stimulate Ca<sup>2+</sup>-induced Ca<sup>2+</sup> release in astrocytic endfeet and amplify neurovascular coupling responses. *Proc Natl Acad Sci U S A*. 2013; 110: 6157–6162. doi: [10.1073/pnas.1216514110](#) PMID: [23530219](#)